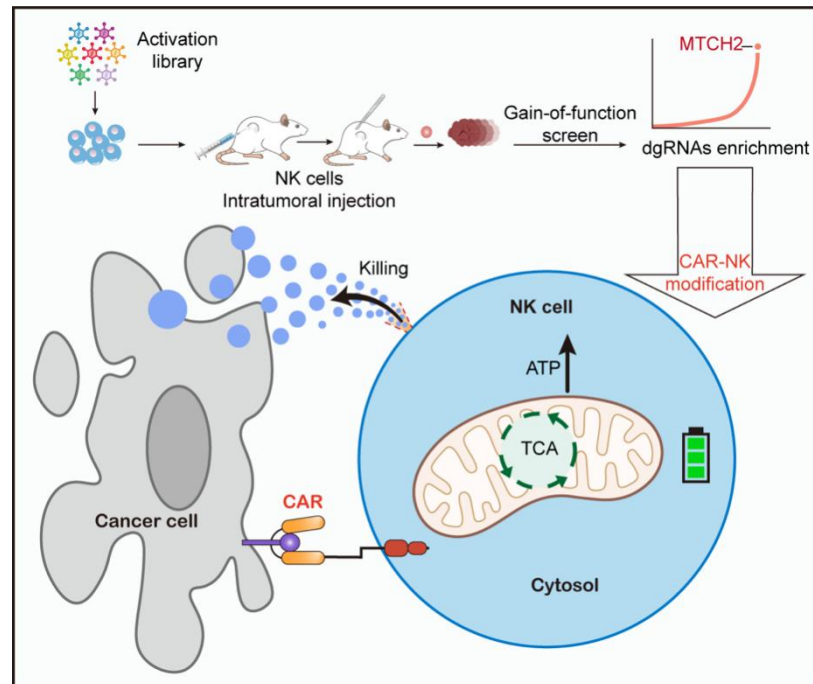


A genome-scale gain-of-function CRISPR screen in NK cells identifies energy metabolism as a means to enhance CAR-NK therapy

Xingrui Qi, Lingyun Kong, Songlin Zhou, Xiaolin Yan, Jianhua Luo & Meng Guo

Graphical abstract



Abstract:

The utilization of chimeric antigen receptor (CAR)-natural killer (NK) cells therapy has shown promise as an immunotherapeutic strategy in combating hematological malignancies. Nevertheless, this therapy encounters various challenges, notably the tumor microenvironment (TME). The identification of an appropriate methodology and molecular target for modifying NK cells to achieve desired functionality under the immunosuppressive pressure of the TME holds significant implications for NK cell-centered therapies. In this study, we employed a CRISPR activation screen library utilizing dead-guide RNA (dgRNA) in NK cells and identified MTCH2, a gain-of-function (GOF) target, notably augmented the functionality and longevity of NK cells in pancreatic cancer. Furthermore, the overexpression of MTCH2 in CAR-NK cells exhibited heightened cytotoxicity in eradicating tumors *in vitro* and *in vivo*. Moreover, MTCH2-overexpression

augmented ATP production, thereby promoting cytotoxicity within the TME. These results collectively establish a screening method for identifying GOF agents for enhancing the efficacy of CAR-NK therapy.

Key words:

CRISPR screen, CAR-NK, MTCH2, directed evolution, solid tumor

Introduction

The implementation of adoptive cell transfer (ACT) therapy has significantly transformed the landscape of cancer treatment. Notably, the utilization of CAR-T cells has yielded extraordinary clinical outcomes in specific subgroups of B cell leukemia or lymphoma. As of now, the Food and Drug Administration (FDA) has granted approval to six distinct CAR-T cell therapies, all of which are designed to target hematological malignancies ¹. Nevertheless, there exist several obstacles that impede the efficacy of CAR-T cell therapy, such as the occurrence of cytokine release storm (CRS), antigen escape, limited trafficking, graft-versus-host disease (GVHD), and restricted tumor infiltration. In contrast, natural killer (NK) cells, being cytotoxic lymphocytes that play a pivotal role in the innate immune system, exhibit advantageous attributes, including potent cytolytic capabilities, a minimal side effects profile, and the ability to recognize targets independent of major histocompatibility complex (MHC) restrictions. Therefore, CAR-NK cells can be generated using peripheral blood (PB) obtained from healthy donors, umbilical cord blood (UCB), induced pluripotent stem cells (iPSCs), or existing NK cell lines. These CAR-NK cells exhibit the ability to eliminate tumor cells via both CAR-dependent and CAR-independent mechanisms, thus presenting a highly promising approach in the field of immunotherapy ².

Till now the efficacy of CAR-T and CAR-NK cells in the treatment of solid tumors is hindered by various factors. These include the heterogeneity of antigen expression in cancer cells, the inherent adaptability of tumors, and the immunosuppressive TME, all of which contribute to the impairment of CAR-T or CAR-NK cell functionality. The senescence of adoptive immune cells may occur due to the deprivation of essential nutrients, variable interstitial fluid pressure, and the presence of hypoxic regions within the TME ³. Furthermore, the interaction between

CAR-host cells and immunosuppressive cells within the TME significantly impacts the functionality of CAR-NK cells ⁴. Consequently, there is an immediate need to identify the appropriate molecular target for the engineering of NK cells, enabling them to adapt to TME pressures, exhibit prolonged lifespan, and exhibit enhanced functionality.

The clustered regularly interspaced short palindromic repeats (CRISPR) system, initially identified in bacteria as a defense mechanism against viral intrusion, utilizes guide RNA (gRNA) to precisely target specific genomic regions and induce double-strand DNA breaks, thereby facilitating gene knockout ⁵. The utilization of a Gain-of-Function (GOF) screen enables the direct identification of functional enhancers that can be utilized for the programming of NK cells. This methodology allows for the targeted identification of specific genes under controlled conditions. In our research project, we conducted an artificial evolution experiment utilizing a genome-scale GOF CRISPR screen lentivirus library, subsequently selecting genes that promote the persistence and antitumor efficacy of NK cells. Ultimately, we discovered that the energy metabolism gene *MTCH2* significantly enhances the cytotoxic capabilities and survival of CAR-NK cells within TME. Together, our findings provide a selection system for identification of GOF immune boosters and demonstrate *MTCH2* as a target to enhance CAR-NK efficacy.

Results

1. Identification of boosters of effector function for NK cells under TME pressure

The solid tumor, particularly pancreatic ductal adenocarcinoma (PDAC), is distinguished by the presence of extracellular matrix, increased levels of soluble suppressive cytokines, modified chemokine expression profiles, hypoxia, and abnormal tumor metabolism ⁶. Consequently, autologous immune cells and adoptively reinfused CAR-NK cells face challenges in effectively infiltrating the solid tumor and performing their functions optimally ⁷. In order to ascertain the genes responsible for enhancing the tumor-killing ability and longevity of NK cells in TME, we employed a genome-scale GOF dgRNA library. This library was incorporated into a lentiviral delivery system and its functionality was quantified through flow cytometry to obtain an adequate viral titer for conducting genome-scale activation screening. Subsequently, NK cells were infected with the lentiviral pool and subcutaneously

administered into the tumor tissue of mice with pancreatic cancer, serving as the initial stress screening environment (Fig. 1A). After a period of 72 hours, the NK cells were gathered and subsequently sorted following library transduction. The sorted NK cells were then subjected to Illumina sequencing in order to determine the abundance of dgRNA throughout the entire library.

Figure 1B demonstrates the identification of significantly enriched dgRNAs in sorted NK cells, targeting 10 genes (MTCH2, METAP1, CHODL, STAT4, CISD1, CCDC68, SLC19A2, SHANK1, DGKZ, and CES5A) based on a false discovery rate (FDR) of 0.1%. The findings of this screening indicate the impartial gain-of-function (GOF) effects of endogenous genes on the survival and persistence of NK cells, thereby providing potential targets for the remodeling of NK cells.

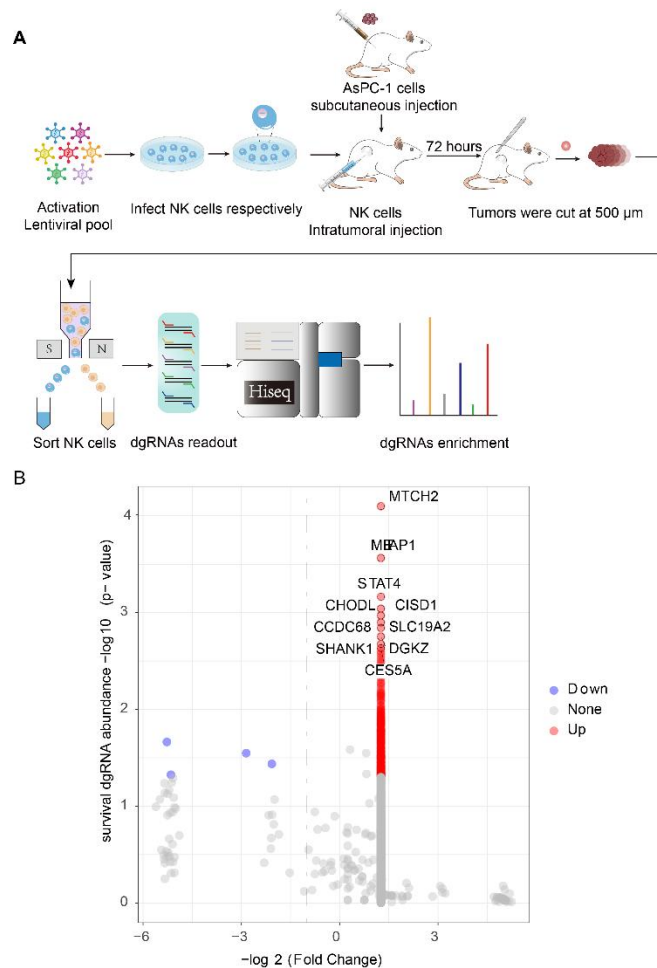


Figure 1 CRISPRa screening has identified MTCH2 as a promising candidate for enhancing NK cell functionality

(A) Schematic diagram of GOF NK cells. AsPC-1 cells were subcutaneously injected into the right flank of NCG mice. 7 days later, lentivirus infected NK cells were intratumorally injected into subcutaneous AsPC-1 xenografts. Collected tumor tissues and sorted NK cells. dgRNAs

enrichment was performed by deep sequencing PCR.

(B) Abundance dgRNA of survived NK cells, including MTCH2, METAP1, CHODL, CISD1, CCDC68, SLC19A2, SHANK1, DGKZ, and CES5A. Red dots, the gene enhanced and passed FDR 0.1% cutoff.

2. The verification of the enhancer's impact on the antitumor efficacy of NK cells in the presence of tumor-induced pressure

The nine genes mentioned above were individually packaged in lentivirus and subsequently used to infect NK cells. The resulting NK cells, which overexpressed different genes, were then co-cultured with K562 cells at an effector to target ratio of 1:1 for a duration of 4 hours, serving as a secondary stress pressure environment. Our findings indicate that NK cells overexpressing MTCH2 demonstrated the highest level of cytotoxicity compared to NK cells overexpressing CCDC68 and other genes (Fig. 2A).

In order to further validate the primary gene that influences the antitumor effectiveness of NK cells combating solid tumors, a mouse model of orthotopic pancreatic cancer was established to simulate the third pressure environment. Subsequently, the aforementioned gene was overexpressed in NK cells and administered to these mice (Fig. 2B). Notably, a reduction in tumor burden was observed across all groups receiving different NK cell treatments, with the MTCH2-overexpressed group exhibiting the most favorable response (Fig. 2C). This finding substantiates the notion that the expression of MTCH2 significantly enhances the *in vivo* tumor-killing activity of NK cells.

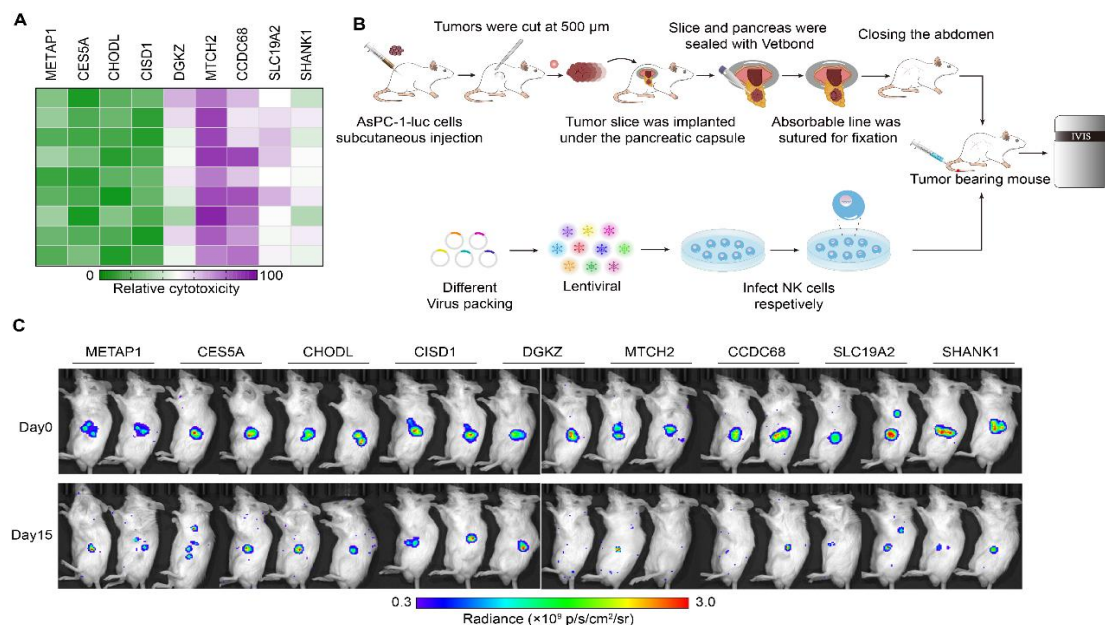


Figure 2 MTCH2 enhances cytotoxicity of NK cells

(A) Heatmap showing the cytolytic activity against K562 cells of MTCH2, METAP1, CHODL, CISD1, CCDC68, SLC19A2, SHANK1, and DGKZ overexpressed NK cells, measured by the LDH assay.

(B) Schematic outline of the development of the modified orthotopic PDAC model and evaluation of antitumor activity of various NK cells. The tumor-bearing mice received different gene overexpressed NK cells respectively.

(C) Tumor aggressiveness was monitored weekly using Living Image software.

3. MTCH2 promotes the function of CAR-NK cells targeting pancreatic cancer

In order to exploit the functionality of MTCH2 in programming NK cells for cell therapy, we employed lentiviral overexpression of MTCH2 construct alongside the second-generation CAR-NK targeting MSLN. The cell surface antigen mesothelin (MSLN) has been identified as a remarkably specific and targetable entity in pancreatic cancers⁸. In order to address MSLN-positive-solid tumors, we generated anti-MSLN CAR-NK92 cells through the utilization of a lentiviral vector that encodes anti-MSLN scFv, 4-1BB, and CD3 ζ as intracellular signaling domains, as well as MTCH2-overexpression. These cells are hereafter referred to as BB ζ or BB ζ -M (Fig. S1). The efficacy of various CAR-NK cells in inducing cytotoxicity was assessed by co-culturing them with AsPC-1 cells, a pancreatic cell line that expresses MSLN. The co-culture data demonstrated that CAR-NK cells with MTCH2 overexpression significantly enhanced the tumor-killing effect, whereas the enhancement effect of NK-92 cells was notably weak (Fig. 3A). Moreover, the present study observed a specific increase in the levels of the potent molecules perforin (PFN) and Granzyme B (GrB) in natural killer (NK) cells that were genetically modified with the BB ζ -M construct, subsequent to co-cultivation with AsPC-1 cells (Fig. 3B-D). Additionally, the expression of the activation marker CD107a in BB ζ -M NK cells was specifically enhanced (Fig. 3E). Collectively, these findings provide evidence that the engineering of MTCH2 enhances the cytotoxicity of antigen-specific chimeric antigen receptor (CAR)-NK cells in an *in vitro* setting.

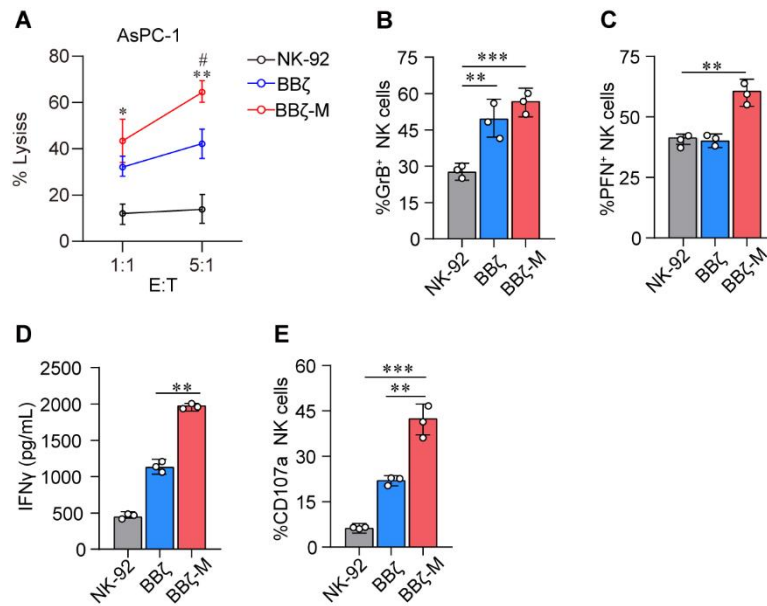


Figure 3 MTCH2 boosts anti-tumor effect of CAR-NK cells

(A) NK-92 cells were co-cultured with target cells (AsPC-1) at the E:T at 1:1. (B-E) GrB expression (B) PFN expression (C) CD107a expression (E) were analyzed in FCS , and IFN- γ production (D) were analyzed by ELISA . Statistical analysis by two-tailed one-way ANOVA (**p < 0.01, ***p < 0.001 compared with NK-92, # p < 0.01 compared with BB ζ) .

4. MTCH2 promotes the persistence of CAR-NK cells in TME

The inhibitory tumor microenvironment (TME) in solid tumors presents challenges for the infiltration of adoptive cells. In this study, we examined the durability of adoptive chimeric antigen receptor (CAR)-natural killer (NK) cells within the tumor tissue of pancreatic cancer (Fig. 4A). Our findings revealed a significantly greater abundance of BB ζ -M NK cells compared to BB ζ NK cells (Fig. 4B). These results suggest that MTCH2 may enhance the longevity of BB ζ NK cells within the TME, consequently supporting their anti-tumor efficacy.

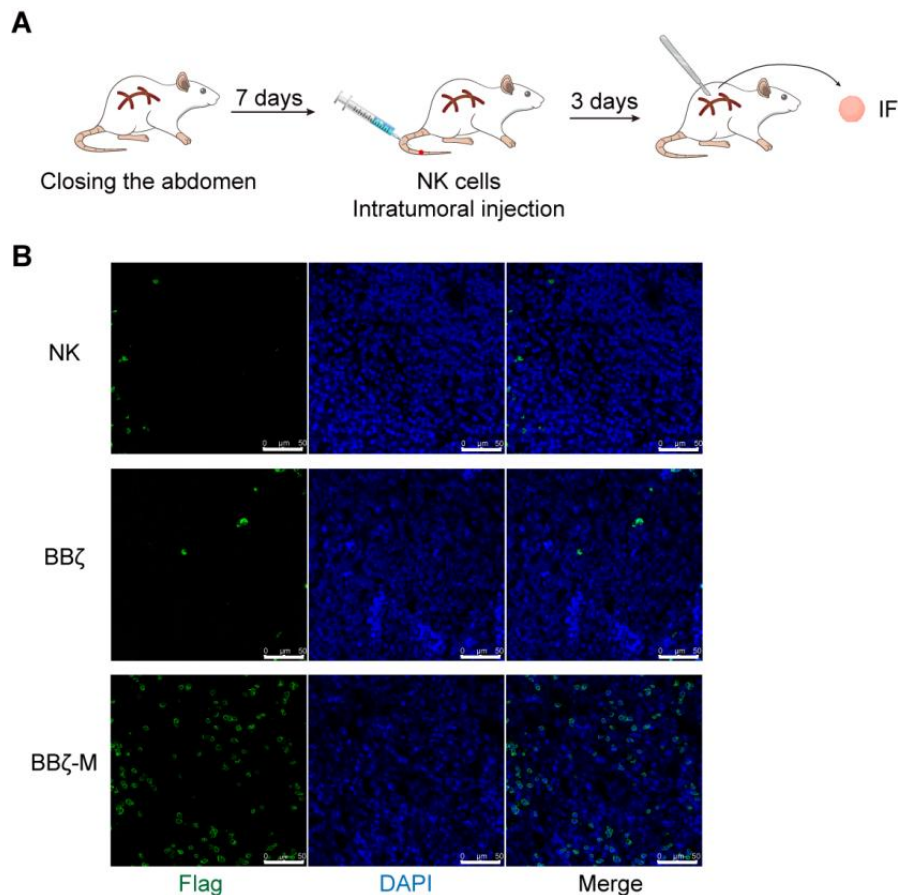


Figure 4 The persistence of BBζ NK cells with TME is enhanced by MTCH2

(A) Schematic representation of tumor model and treatment.

(B) Orthotopic models of pancreatic cancer were established in mice. NK-92, BBζ cells or BBζ-M NK cells (1×10^7 /mouse) were injected in mice via tail vein on day 7, 14 and 21 after tumor establishment. After adoptive infusion, tumor samples were obtained for intra-tumor survival of BBζ NK or BBζ-M NK cells by IF.

5. MTCH2 engineering enhances antitumor efficacy of CAR-NK *in vivo* against various animal models

To further evaluate the augmentation of antitumor activity through MTCH2 overexpression, we proceeded to create diverse MTCH2-overexpressed CAR-NK cells that targeted different tumor models. Specifically, we established subcutaneous tumor-bearing mice encompassing esophageal cancer, hepatocellular carcinoma, and cholangiocarcinoma (Fig. 5A). Subsequently, NK-92, BBζ, or BBζ-M NK cells were individually administered. The analysis of tumor growth kinetics demonstrated that BBζ-M cells exhibited a substantial improvement in efficacy when compared to NK-92 and BBζ NK cells. Notably, treatment with BB-M NK cells led to the most pronounced reduction in tumor growth, as depicted in Figure 5 B-D. These findings

provide evidence that MTCH2 enhances the effectiveness of BB ζ NK cells in combating diverse solid tumors in an *in vivo* setting.

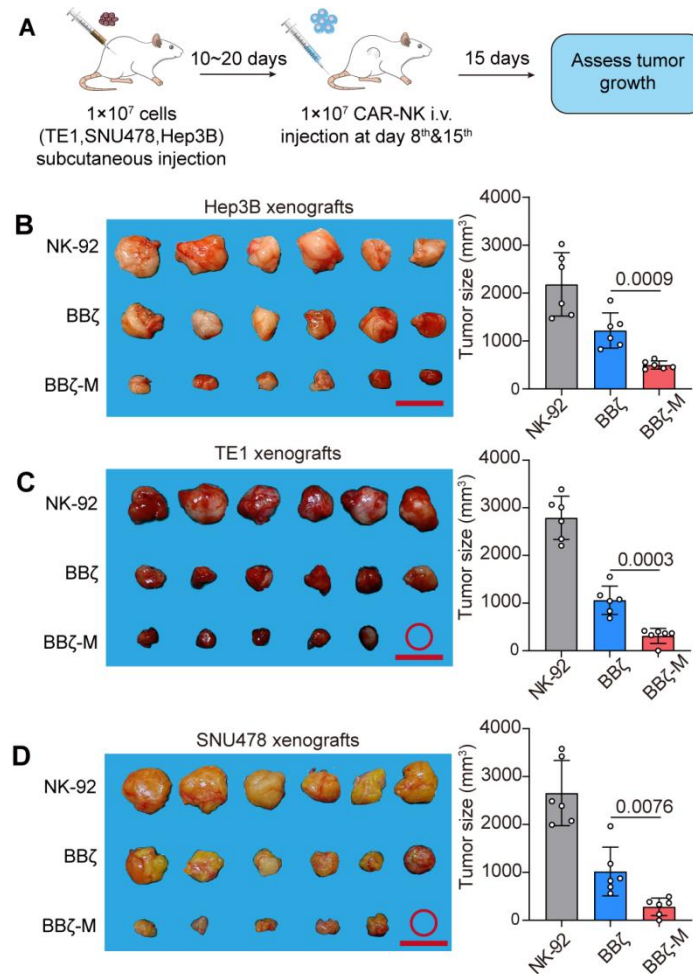


Figure 5 MTCH2 enhances the antitumor efficacy of different CAR-NK cells *in vitro*

(A) Schematic representation of tumor models and treatment. Tumors were established by subcutaneous injection of TE1/SNU478/Hep3B cells. 10 days later, murine were treated with NK-92/BB ζ /BB ζ -M NK cells. 21 days after tumor established, tumor growth was assessed.

(B-D) Tumor size of Hep3B, TE1 and SNU478 mice models at 21 days post-treatment (n=6 each). Scale bars are 2 cm. Statistical analysis by two-tailed one-way ANOVA .

6. MTCH2 enhances the ATP generation of CAR-NK cells

MTCH2 was determined to be both essential and adequate for the incorporation of various α -helical proteins into the outer membrane of the mitochondria. The absence of MTCH2 has been linked to a range of multifaceted characteristics, such as impairments in mitochondrial fusion and the maintenance of mitochondrial mass, which are crucial for energy production ⁹. Consequently, we hypothesized that MTCH2 could augment the anti-tumor capabilities of targeting solid tumors by

increasing ATP generation in TME. An ATP generation assay was performed to provide evidence that MTCH2 over-expressed BB ζ NK cells exhibited higher ATP production compared to the other group (Fig. 6A), suggesting a significant involvement of MTCH2 in ATP generation.

The TCA cycle is responsible for the production of ATP through OXPHOS¹⁰. Subsequently, we evaluated the extent of OXPHOS by quantifying the rate of cellular oxygen consumption (OCR) and observed a substantial increase in mitochondrial maximal respiration in BB ζ -M NK cells (Fig. 6B-C). These findings suggest the significance of MTCH2 in augmenting the functionality of CAR-NK cells.

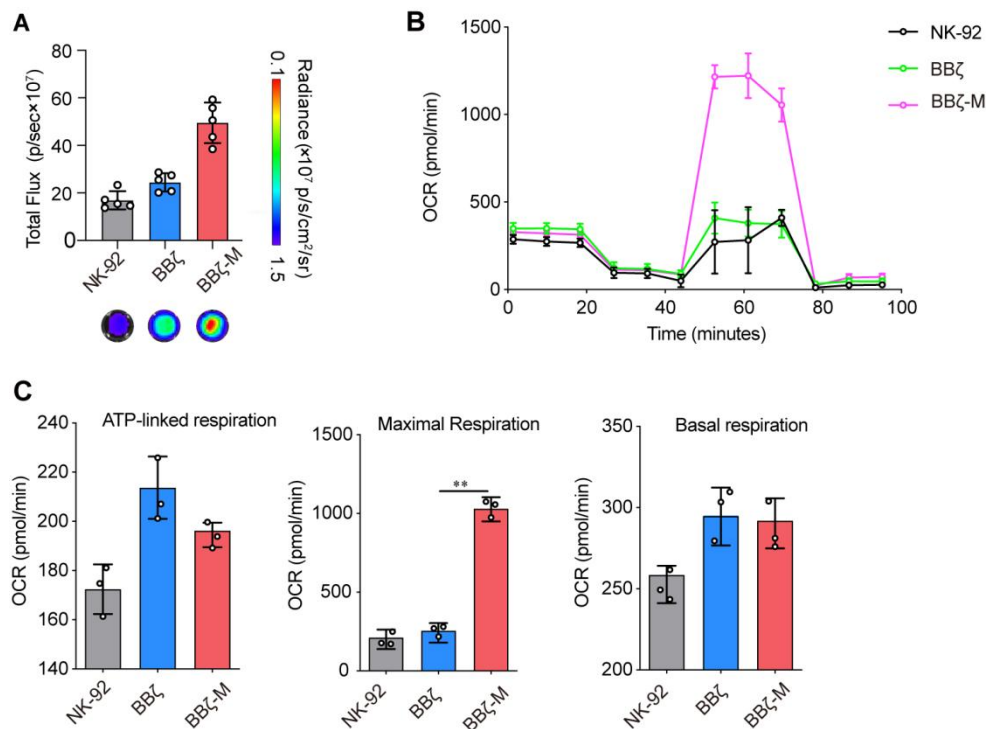


Figure 6 MTCH2 enhances OXPHOS of BB ζ NK cells

(A) ATP generation in NK-92, BB ζ and BB ζ -M NK cells after co-cultured with AsPC-1 cells for 4 hours.

(B-C) OCR in NK-92, BB ζ and BB ζ -M NK cells after co-cultured with AsPC-1 cells for 4 hours. Statistical analysis by two-tailed one-way ANOVA (**p < 0.01 compared with NK-92).

Discussion

The urgent task addressing the inhibitory effects within TME arises as immune cells emerge as potential therapeutic avenues for cancer immunotherapy. The attainment of a resilient metabolic state in immune cells is imperative for the execution of anti-tumor effector functions¹¹. However, cancer cells exhibit robust

metabolic activity and excel in nutrient uptake. The inadequate metabolic performance of NK cells within the TME, including impaired energy generation, has been demonstrated to compromise their immune surveillance capabilities¹². To augment the infiltration, and viability of adoptive immune cells within solid tumors, previous investigation successfully engineered CAR-T cells generating IL-7 and CCL19¹³. The integration of CAR-NK cells with oncolytic virus expressing cytokine demonstrated robust antitumor reactions¹⁴. However, these approaches failed to address the challenges pertaining to the sustenance of immune cells in TME, particularly in terms of energy supply and cell survival.

In this study, our objective is to employ CRISPR screen methodology to identify the pivotal molecule capable of overcoming the immunosuppressive TME and subsequently utilize this gene in cellular immunotherapy. To achieve this, we have devised three artificial screening pressures. Initially, we established a subcutaneous tumor-bearing mouse model of pancreatic cancer. Subsequently, we intratumorally injected NK cells infected with a GOF library into the tumor tissue, allowing for the selection of genes that exhibit resistance to the TME and enhance the survival of NK cells. Subsequently, we conducted a co-culture experiment involving NK cells that were genetically modified to overexpress the aforementioned genes, in conjunction with pancreatic cancer tumor cells. This experimental setup served as a secondary screening environment, aimed at identifying genes that could facilitate the efficient secretion of effector molecules by NK cells under pressure. It is worth noting that pancreatic cancer is widely recognized as the most aggressive solid tumor, primarily due to its unfavorable prognosis, high mortality rate, and unique TME. Consequently, a mouse model of pancreatic cancer bearing orthotopic tumors was established as the third screening pressure. The genes of interest identified under the initial stress condition were subsequently upregulated in NK cells, which were then reintroduced into tumor-bearing mice to identify the gene that could effectively impede the growth of pancreatic cancer. Ultimately, we confirmed that MTCH2 is crucial for the cytotoxic activity of NK cells, and subsequently utilized it in the development of CAR-NK cells.

MTCH2 is an integral membrane protein, function in facilitating the transport of metabolites into the mitochondrial matrix. Depletion of MTCH2 has been linked to a range of multifaceted characteristics, encompassing impairments in mitochondrial

fusion, and apoptosis¹⁵. Considering the significance of mitochondria as essential organelles in the metabolic reprogramming, we propose that targeting mitochondria could revolutionize future approaches to cancer treatment. Within our study, we have observed that the overexpression of MTCH2 substantially augments the anti-tumor efficacy of diverse CAR-NK cells that target various tumor associated antigens (TAA). Consequently, our findings not only offer a means for identifying GOF immune enhancers but also establish a basis for further advancements in the engineering of CAR-NK cells to attain superior functionality.

Methods

Mice and cell lines

Female NOD/ShiltJGpt-Prkdc^{em26Cd52}Il2rg^{em26Cd22}/Gpt (NCG) mice were purchased from Gempharmatech Inc (Nanjing, China) and kept in specific pathogen-free conditions. Mice experiments were approved by the Scientific Investigation Board of Navy Medical University (Shanghai, China). NK-92, AsPC-1 and K562 cells as we previously described¹⁶. The tumor cells were gifts from Department of Pathology, Changhai Hospital, Navy Medical University. The tumor cells were grown in DMEM (Gibco), 10% fetal bovine serum (FBS). All cell lines tested negative for Mycoplasma.

Establishment of Orthotopic Pancreatic Cancer Murine Models

The tumor graft was obtained by inoculating AsPC-1-luc cells subcutaneously into the right hind limbs of NCG mice (2×10^7 cells in each mouse) at 6 weeks of age¹⁷. As the tumor reached a diameter of about 8 to 10 mm after tumor seeding, the mice were euthanized by cervical dislocation and tumor tissue was taken from the mice. After obtaining tumor samples, UW (University of Wisconsin) preservation solution was immediately applied. Following that, each tumor was wrapped in 5% low-melt agar and quickly sectioned with a tissue slicer at a thickness of 500 μ m. As soon as the sections were obtained, they were immediately transferred to ice-cold UW solution. Using ophthalmic scissors, a 1 cm port was cut above the spleen, followed by the gentle squeeze out of the pancreas tail using atraumatic forceps. A tumor slice was carefully inserted into the subcapsular space after blunt dissection of the capsule of the pancreas. Vetbond (3M, 1469SB) was used to attach the graft to the pancreas,

followed by 5-0 absorbable sutures for reinforcement. In the end, the abdominal cavity was closed after the spleen and pancreas were incorporated into it.

Lentivirus production

Lentivirus production was achieved by utilizing lenti-X-293 cells¹⁸. The day prior to transfection, lenti-X-293 cells were seeded in 15 cm-dish at the confluency of 70-80%. The media was substituted with 10.5 mL pre-warmed DMEM medium (Invitrogen) 2 hours before transfection. To each plate, the medium was mixed with pLVX-EF1a-IRESpuro or vector control plasmid, pCMVR8.74, pMD2.G and polybrene. Following a brief vortex, the mixture was incubated for 15 minutes at room temperature and then added drop by drop slowly to cells. 6 hours later, DMEM media was substituted with 20 mL pre-warmed DMEM media. Viral supernatant was gathered at 48 hours and 72 hours after transfection, subsequently filtered with a 0.40 mm filter (Fisher / VWR) to eliminate cell debris, and finally concentrated using AmiconUltra 100 kD ultracentrifugation units (Millipore). The virus was divided into smaller portions and stored at -80 °C.

Library Virus Infection Experiment

Infect $5 \times 10^7 \sim 1 \times 10^8$ cells (245 mm \times 245 mm plate to spread cells) with lentivirus at the functional MOI=0.4. Meanwhile, set up 2 parallel infection experiments as well as a blank control group (virus-free). 5 samples should be collected during the experiment, i.e. data on day 0 of control group, day 7 of control group and experimental group, day 14 of control group. Add the appropriate concentration of hygromycin B to each plate. When the control group is completely killed, digest the cells and collect at least 3×10^7 cells (this is the control sample on day 0, and about 200 μ g of the genome can be extracted). The genomic DNA was extracted with the Tigen Genome Extraction Kit and the remaining cells were divided into two groups in equal amounts. Add the Vehicle and target drug to screen (each has 3 replicate wells) 2 days after passaging (after wall attachment). Collect the genome of the cells on day 7 and day 14 after drug treatment. Extract the cells genome and perform quality control.

Tumor Tissue Dissociation

On day 21 after tumor inoculation, the mice were euthanized by cervical

dislocation and tumor tissue was harvested. Cut tissue sample and digested by digestive solution (2.5 mg/ml type II collagenase and 10 μ M Y-27632). Incubated tumor sample at 37°C in the shaking incubator for thorough digestion about 1 hour until no obvious large tissue could be found. Then the digestion was filtrated by a 70 μ m filter. The obtained filtrate was centrifuged at 1500 rpm for 5 min. Discarded the supernatant and added 3-5 mL of terminal culture media, centrifuged at 1500 rpm for 5 min. At last, used tumor culture media to resuspend cells.

Sort NK cells

Cells were collected and rinsed once using MACS buffer (0.5 % BSA and 2 mM EDTA in PBS). The NK cells were subsequently sorted by MojoSort™ Human NK Cell Isolation Kit (Biolegend, 480054).

CRISPR screening

Total RNA isolation, RNA quality control, library construction, sequencing and data analysis were performed by Shanghai Biotechnology Corporation (Shanghai, China). Phusion Flash High Fidelity Master Mix (Thermo Fisher) to perform two-step PCR amplification for dgRNA readout. PCR #1 used primers to amplify dgRNA Cassette:

Forward: 5'-AATGGACTATCATATGCTTACCGTAACTTGAAAGTATTTTCG-3'

Reverse: 5'AACGTTACGGCGACTACTGCACTTATATACGGTTCTC-3'

PCR #2 used uniquely barcoded primers:

Forward: 5'-TCTTGTGGAAAGGACGAAACACC-3'

Reverse: 5'-GCCAAGTTGATAACGGACTAGCCTT-3'

CAR-NK-92 Cell Line Establishment

Seed NK-92 cells at 1×10^5 per well in a 24-well plate. Mix 2 mg/mL of polybrene per well, and add 2 mg/mL of polybrene per well, mix thoroughly, and add the encapsulated virus at different MOI values (1, 10, 50, 100, 500, 1000). After 12 hours of infection, all the cells were aspirated and transferred to 25 cm² containing 9 mL of complete culture medium. The percentage of CAR-positive cells was detected by FACS. The cells were collected by centrifugation at 3000 rpm for 5 min. Discard the supernatant and add ice-cold PBS 1 mL to wash the cells once. Cells were resuspended in 50 μ L PBS and 2 μ L of FLAG-APC antibody (BioLegend, 637308)

was added. Incubate NK cells at room temperature for 15 min, add 1 mL of ice-cold PBS and centrifuge at 3000 rpm for 5 min to collect the cells. Add 1 mL ice-cold PBS and wash the cells once, discard the supernatant and add 50 μ L ice-cold PBS to resuspend the cells for flow assay. Cells with the highest CAR positivity rate and cell viability of not less than 95% are selected for expansion and sorting. The cells were sorted after proliferation to 10^7 and the cells were centrifuged at 1500 rpm for 5 min, and washed once with 30 mL of ice-cold PBS. Cells were resuspended in 200 μ L PBS, labeled with 10 μ L of sterile FLAG-APC antibody (BioLegend, 637308), then incubated for 15 min away from light. The cells were washed with 30 mL of ice-cold PBS and the supernatant was well discarded. 500 μ L PBS was used to resuspend the cells. Positive cells were sorted. Sorted cells were cultured in 24-well plates, expanded and get subclone.

Construction of AsPC-1 subcutaneous tumor model

5×10^6 AsPC-1 cells in 50 μ L of HBSS were injected via subcutaneous injection into the right flank of NCG mice. NK cells were treated with mitomycin-C to inhibit their proliferation Then intratumorally injected into subcutaneous AsPC-1 xenografts. After 72 hours, the persistence of NK cells in tumor tissues was collected and determined by immunofluorescence (IF).

IF

Tumor tissues were formalin-fixed and paraffin-embedded. Incubated with fluorescence-conjugated antibody targeting CD56 (NCAM1 (CD56) (E7X9M) Rabbit mAb, CST, 99746). Then, incubated with fluorescence conjugated antibodies. Images were captured with a 63 \times /1.4-NA oil-immersion objective. Leica confocal software (Leica, Germany) was used to process images.

ELISA

4 hours co-culture of NK cells with tumor cells, the supernatant was collected and analyzed using the quantikine ELISA human IFN- γ Immunoassay according to the manufacturer's instructions. A microplate reader (PerkinElmer, Waltham, MA, USA) was used to read the 96-well plates at 450 nm.

Cytotoxicity assay

For lactate dehydrogenase (LDH), CytoTox96 cytotoxicity assay was used according to the manufacturer's instructions. Briefly, target cells were plated in NK cells media in white-walled 96-well plates, followed by the addition of NK cells at E:T ratio=1:1 or 5:1. Finally, cytotoxicity was calculated based on LDH release using the following formula: Cytotoxicity (%) = $[\text{LDH}^{\text{E:T}} - \text{LDH}^{\text{E}}] / \text{LDH}^{\text{Max}} \times 100\%$. Specific steps as we previously described ¹⁹.

ATP generation assay

ATP generation analyzed using the Luminescent Cell Viability Assay according to the manufacturer's instructions. In brief, thaw the CellTiter-Glo reagent and equilibrate to RT. Add the test compound to experimental wells, then add equivalent volume CellTiter-Glo Reagent to the cell culture medium present in each well. Agitate the mixture for 2 minutes on an orbital shaker to initiate the lysis of cells. Total luminescence signal was quantified using Living Image software (Perkin Elmer).

Seahorse metabolic assays

Specific steps as previously described ²⁰ and analyzed on an Agilent Seahorse XF 24-well analyzer. Briefly, after co-cultured with tumor cells, NK-92, BB ζ cells and BB ζ -M NK cells were seeded at 2×10^5 per well in cell culture microplates pre-coating with poly-lysine. Cells were equilibrated for 1 hour in XF assay medium supplemented with 10 mM glucose, 1 mM sodium pyruvate and 2 mM glutamine in a non-CO₂ incubator. OCR were monitored at baseline and throughout sequential injections of oligomycin (1.5 μM), carbonyl cyanide-4-(trifluoromethoxy) phenylhydrazone (0.5 μM) and rotenone or antimycin A (0.5 μM each).

Statistical analysis

GraphPad Prism 8.0 was used for all statistical analyses. A two-tailed unpaired student t-test was used to determine significance. One-way analysis of variance (ANOVA) with a Bonferroni post-test was used to compare differences among multiple groups. Survival analysis was performed by KaplanMeier survival analysis.

Acknowledgments

This work was supported by grants from the National Natural Science Foundation of China (82071799), and National Key Basic Research Program of China (20ZR1469900). We sincerely thank the supports from National Key Laboratory of Immunity & Inflammation, Institute of Immunology, Navy Medical University.

Competing Interests

The authors declare no competing interests.

References

1. Stirrups, R., CAR T-cell therapy for relapsed or refractory mantle-cell lymphoma. *Lancet Oncol* **2020**, *21* (5), e239.
<https://www.nejm.org/doi/10.1056/NEJMoa1914347>
2. Myers, J. A.; Miller, J. S., Exploring the NK cell platform for cancer immunotherapy. *Nat Rev Clin Oncol* **2021**, *18* (2), 85-100.
<https://www.nature.com/articles/s41571-020-0426-7>
3. Majzner, R. G.; Mackall, C. L., Tumor Antigen Escape from CAR T-cell Therapy. *Cancer Discov* **2018**, *8* (10), 1219-1226.
<https://aacrjournals.org/cancerdiscovery/article/8/10/1219/6227/Tumor-Antigen-Escape-from-CAR-T-cell>
4. Sterner, R. C.; Sterner, R. M., CAR-T cell therapy: current limitations and potential strategies. *Blood Cancer J* **2021**, *11* (4), 69.
<https://www.nature.com/articles/s41408-021-00459-7>
5. Knott, G. J.; Doudna, J. A., CRISPR-Cas guides the future of genetic engineering. *Science* **2018**, *361* (6405), 866-869.
<https://www.science.org/doi/10.1126/science.aat5011>
6. Whiteside, T. L., The tumor microenvironment and its role in promoting tumor growth. *Oncogene* **2008**, *27* (45), 5904-12.
<https://www.nature.com/articles/onc2008271>
7. Gajewski, T. F.; Schreiber, H.; Fu, Y. X., Innate and adaptive immune cells in the tumor microenvironment. *Nat Immunol* **2013**, *14* (10), 1014-22.
<https://www.nature.com/articles/ni.2703>
8. Kindler, H. L.; Novello, S.; Bearz, A.; Ceresoli, G. L.; Aerts, J. G.; Spicer, J.; Taylor, P.; Nackaerts, K.; Greystoke, A.; Jennens, R., Anetumab

ravtansine versus vinorelbine in patients with relapsed, mesothelin-positive malignant pleural mesothelioma (ARCS-M): a randomised, open-label phase 2 trial. *The Lancet Oncology* **2022**, 23 (4), 540-552.

<https://linkinghub.elsevier.com/retrieve/pii/S1470204522000614>

9. Aman, Y.; Erinjeri, A. P.; Tataridas-Pallas, N.; Williams, R.; Wellman, R.; Chapman, H.; Labbadia, J., Loss of MTCH-1 suppresses age-related proteostasis collapse through the inhibition of programmed cell death factors. *Cell Rep* **2022**, 41 (8), 111690.

<https://linkinghub.elsevier.com/retrieve/pii/S2211124722015649>

10. Su, L.; Zhang, J.; Gomez, H.; Kellum, J. A.; Peng, Z., Mitochondria ROS and mitophagy in acute kidney injury. *Autophagy* **2023**, 19 (2), 401-414.

<https://www.tandfonline.com/doi/full/10.1080/15548627.2022.2084862>

11. Leone, R. D.; Powell, J. D., Metabolism of immune cells in cancer. *Nat Rev Cancer* **2020**, 20 (9), 516-531.

<https://www.nature.com/articles/s41568-020-0273-y>

12. Zhu, M.; Barbas, A. S.; Lin, L.; Scheuermann, U.; Bishawi, M.; Brennan, T. V., Mitochondria Released by Apoptotic Cell Death Initiate Innate Immune Responses. *Immunohorizons* **2019**, 3 (1), 26-27.

<https://journals.aai.org/immunohorizons/article/2/11/384/3905/Mitochondria-Released-by-Apoptotic-Cell-Death>

13. Adachi, K.; Kano, Y.; Nagai, T.; Okuyama, N.; Sakoda, Y.; Tamada, K., IL-7 and CCL19 expression in CAR-T cells improves immune cell infiltration and CAR-T cell survival in the tumor. *Nature biotechnology* **2018**, 36 (4), 346-351.

<https://www.nature.com/articles/nbt.4086>

14. Rezaei, R.; Esmaili Gouvarchin Ghaleh, H.; Farzanehpour, M.; Dorostkar, R.; Ranjbar, R.; Bolandian, M.; Mirzaei Nodooshan, M.; Ghorbani Alvanegh, A., Combination therapy with CAR T cells and oncolytic viruses: a new era in cancer immunotherapy. *Cancer Gene Ther* **2022**, 29 (6), 647-660.

<https://www.nature.com/articles/s41417-021-00359-9>

15. Guna, A.; Stevens, T. A.; Inglis, A. J.; Replogle, J. M.; Esantsi, T. K.; Muthukumar, G.; Shaffer, K. C. L.; Wang, M. L.; Pogson, A. N.; Jones, J. J.; Lomenick, B.; Chou, T. F.; Weissman, J. S.; Voorhees, R. M., MTCH2 is a mitochondrial outer membrane protein insertase. *Science* **2022**, 378 (6617), 317-322.

<https://www.science.org/doi/10.1126/science.add1856>

16. Guo, M.; Sun, C.; Qian, Y.; Zhu, L.; Ta, N.; Wang, G.; Zheng, J.; Guo, F.; Liu, Y., Proliferation of highly cytotoxic human natural killer cells by OX40L armed NK-92 with secretory neoleukin-2/15 for cancer immunotherapy. *Frontiers in Oncology* **2021**, *11*, 632540.

<https://www.frontiersin.org/journals/oncology/articles/10.3389/fonc.2021.632540/full>

17. Erstad, D. J.; Sojoodi, M.; Taylor, M. S.; Ghoshal, S.; Razavi, A. A.; Graham-O'Regan, K. A.; Bardeesy, N.; Ferrone, C. R.; Lanuti, M.; Caravan, P.; Tanabe, K. K.; Fuchs, B. C., Orthotopic and heterotopic murine models of pancreatic cancer and their different responses to FOLFIRINOX chemotherapy. *Dis Model Mech* **2018**, *11* (7).

<https://journals.biologists.com/dmm/article/11/7/dmm034793/53324/Orthotopic-and-heterotopic-murine-models-of>

18. Wang, X.; McManus, M., Lentivirus production. *J Vis Exp* **2009**, (32).

<https://www.jove.com/cn/t/1499/lentivirus-production>

19. Sun, W.; Shi, J.; Wu, J.; Zhang, J.; Chen, H.; Li, Y.; Liu, S.; Wu, Y.; Tian, Z.; Cao, X., A modified HLA-A* 0201-restricted CTL epitope from human oncoprotein (hPEBP4) induces more efficient antitumor responses. *Cellular & Molecular Immunology* **2018**, *15* (8), 768-781.

<https://www.nature.com/articles/cmi2017155>

20. Shi, Q.; Shen, Q.; Liu, Y.; Shi, Y.; Huang, W.; Wang, X.; Li, Z.; Chai, Y.; Wang, H.; Hu, X., Increased glucose metabolism in TAMs fuels O-GlcNAcylation of lysosomal Cathepsin B to promote cancer metastasis and chemoresistance. *Cancer Cell* **2022**, *40* (10), 1207-1222. e10.

<https://linkinghub.elsevier.com/retrieve/pii/S1535610822003762>